Journal for ImmunoTherapy of Cancer

TCR-engaging scaffolds selectively expand antigen-specific T-cells with a favorable phenotype for adoptive cell therapy

Siri Amanda Tvingsholm,[1] Marcus Svensson Frej,[2] Vibeke Mindahl Rafa,[1] Ulla Kring Hansen,[2] Maria Ormhøj,[1] Alexander Tyron,[1] Agnete W P Jensen ,[3] Mohammad Kadivar ,[1] Amalie Kai Bentzen,[1] Kamilla K Munk,[1] Gitte N Aasbjerg,[1] Jeppe S H Ternander,[2] Christina Heeke,[1] Tripti Tamhane,[1] Christian Schmess ,[4] Samuel A. Funt,[5] Julie Westerlin Kjeldsen,[3] Anders Handrup Kverneland ,[3] Özcan Met,[6] Arianna Draghi ,[3] Søren Nyboe Jakobsen,[1] Marco Donia ,[3] Inge Marie Svane,[3] Sine Reker Hadrup [1]

To cite: Tvingsholm SA, Frej MS, Rafa VM, *et al*. TCR-engaging scaffolds selectively expand antigen-specific T-cells with a favorable phenotype for adoptive cell therapy. *Journal for ImmunoTherapy of Cancer* 2023;**11**:e006847. doi:10.1136/jitc-2023-006847

► Additional supplemental material is published online only. To view, please visit the journal online (http://dx.doi.org/10.1136/jitc-2023-006847).

Accepted 16 July 2023

For numbered affiliations see end of article.

Correspondence to
Professor Sine Reker Hadrup; sirha@dtu.dk

ABSTRACT

Background Adoptive cell therapy (ACT) has shown promising results for the treatment of cancer and viral infections. Successful ACT relies on ex vivo expansion of large numbers of desired T-cells with strong cytotoxic capacity and in vivo persistence, which constitutes the greatest challenge to current ACT strategies. Here, in this study, we present a novel technology for ex vivo expansion of antigen-specific T-cells; artificial antigen-presenting scaffolds (Ag-scaffolds) consisting of a dextran-polysaccharide backbone, decorated with combinations of peptide-Major Histocompatibility Complex (pMHC), cytokines and co-stimulatory molecules, enabling coordinated stimulation of antigen-specific T-cells.

Methods The capacity of Ag-scaffolds to expand antigen-specific T-cells was explored in ex vivo cultures with peripheral blood mononuclear cells from healthy donors and patients with metastatic melanoma. The resulting T-cell products were assessed for phenotypic and functional characteristics.

Results We identified an optimal Ag-scaffold for expansion of T-cells for ACT, carrying pMHC and interleukin-2 (IL-2) and IL-21, with which we efficiently expanded both virus-specific and tumor-specific CD8+ T cells from peripheral blood of healthy donors and patients, respectively. The resulting T-cell products were characterized by a high frequency of antigen-specific cells with high self-renewal capacity, low exhaustion, a multifunctional cytokine profile upon antigen-challenge and superior tumor killing capacity. This demonstrates that the coordinated stimuli provided by an optimized stoichiometry of TCR engaging (pMHC) and stimulatory (cytokine) moieties is essential to obtain desired T-cell characteristics. To generate an 'off-the-shelf' multitargeting Ag-scaffold product of relevance to patients with metastatic melanoma, we identified the 30 most frequently recognized shared HLA-A0201-restricted melanoma epitopes in a cohort of 87 patients. By combining these in an Ag-scaffold product, we were able to expand tumor-specific T-cells from 60–70% of patients with melanoma, yielding a multitargeted T-cell product with up to 25% specific and phenotypically and functionally improved T cells.

Conclusions Taken together, the Ag-scaffold represents a promising new technology for selective expansion of antigen-specific CD8+ T cells directly from blood, yielding a highly specific and functionally enhanced T-cell product for ACT.

WHAT IS ALREADY KNOWN ON THIS TOPIC

⇒ Ex vivo expansion of endogenous tumor-specific T-cells from blood represents a promising alternative strategy to rapidly expanded tumor-infiltrating lymphocytes for adoptive cell therapy in cancer. However, most existing technologies fail to selectively target antigen-specific T-cells and represent very complex structures and cumbersome procedures.

WHAT THIS STUDY ADDS

⇒ This study presents a simple and highly flexible new technology to mediate coordinated stimulation of antigen-specific T-cells to drive their selective expansion from blood peripheral blood mononuclear cells (PBMCs). Using the antigen-presenting scaffolds (Ag-scaffold) technology, we can expand both virus-specific and tumor-specific T cells from healthy donors and patient PBMCs, resulting in T-cell products with favorable phenotypic and functional characteristics.

HOW THIS STUDY MIGHT AFFECT RESEARCH, PRACTICE OR POLICY

⇒ This study demonstrates the importance of precise and coordinated stimulation of T cells to achieve favorable characteristics. The Ag-scaffold technology has direct applicability in adoptive cell therapy strategies for treatment of cancer.

INTRODUCTION

Adoptive cell therapy (ACT) in cancer involves the ex vivo expansion and potential enrichment of tumor-reactive T cells, derived from an endogenous source (tumor or

peripheral blood) or from genetic modification of autologous lymphocytes (with synthetic T-cell receptor (TCR) or chimeric antigen receptor (CAR)).[1] Genetically engineered T-cell therapies have provided remarkable clinical success in several hematological malignancies, such as acute lymphoblastic leukemia. However, their achievement in solid tumors is limited since they typically only target a single antigen and are associated with great risk of severe or fatal adverse effects due to increased target affinity and cross-reactivity.[2] In contrast, endogenous T-cell therapies are considered safer, since endogenous cells have gone through negative selection and thus are unlikely to cross-react with healthy cells.[3]

ACT based on autologous tumor infiltrating lymphocytes (TILs; TIL-ACT) has shown promising results in various malignancies, particularly in metastatic melanoma, where phase III data has demonstrated improved progression-free survival compared with standard immune checkpoint inhibition (NCT02278887).[4] Despite the clinical success of TIL-ACT, the current cell manufacturing protocols have limitations. The process is lengthy and includes a massive unselective T-cell expansion step, that drives T cells towards a terminally differentiated and exhausted state.[5 6] This negatively influences the (poly) functionality and persistence of infused T cells which is critical for achieving successful clinical outcome.[7]

Although tumor biopsies are considered a rich source of tumor-reactive T cells, recent reports have shown that the majority of TILs are bystander T cells.[8] Consistently, TIL expansion has been shown to preferentially expand co-infiltrated virus-specific T cells, resulting in clinical-grade TIL infusion products containing only a fraction of tumor-reactive T cells.[9] Finally, TIL-ACT is only applicable to the minority of patients who are able to undergo surgical resection of a metastatic lesion and many TIL cultures fail to yield a usable infusion product, in particular when extending to solid cancers other than melanoma.

To circumvent these challenges and provide an alternative source of tumor-reactive T-cells for ACT, we here pursue the expansion of endogenous tumor-reactive T-cells to therapeutic levels from peripheral blood mononuclear cells (PBMCs). Circulating tumor-reactive T-cells do not reside in the immune-suppressive tumor environment with exposure to chronic TCR stimulation; thus, they are potentially less functionally impaired.[10] Recent data suggest that the majority of tumor-specific T-cells responsible for tumor-rejection under checkpoint inhibitor therapy are recruited from the peripheral blood and lymphatic system, while not being present in the tumor prior to treatment.[11]

Circulating tumor-reactive T-cells are rare and their selective expansion requires targeted delivery of growth and co-stimulatory signals, while limiting bystander proliferation. To achieve this, we designed a simple and easily modifiable antigen-presenting scaffold (Ag-scaffold) for the selective stimulation of antigen-specific T-cells ex vivo. The Ag-scaffold is composed of a dextran polysaccharide backbone, to which any functional molecule can be attached via streptavidin-biotin interactions. Dextran is an attractive biomaterial, since it is naturally biodegradable and already widely used in commercial drug formulations.[12] Here we have focused on Ag-scaffolds carrying the three fundamental signals required for optimal T-cell activation: peptide-Major Histocompatibility Complex (pMHC) complexes for specific TCR engagement, co-stimulatory molecules (eg, B7.2) and cytokines (eg, interleukin (IL)-15, IL-2 and IL-21)[13]. This Ag-scaffold is designed to bind specific T-cells via pMHC-TCR interaction and provide fine-tuned co-stimulatory and growth signals exclusively to pMHC-engaged T-cells. Interestingly, we observe that the coordinated interaction of both TCR-engaging and T-cell stimulatory signals is required to expand T-cells with stem-like phenotypic characteristics.

Other strategies have been pursued to obtain selective expansion of antigen-specific T-cells. These include patient-derived autologous dendritic cells (DCs) pulsed or transfected with antigens of interest; however, the generation of autologous DCs is prone to variability depending on patient characteristics and cumbersome handling procedures.[14] In an effort to overcome these challenges, various cellular and acellular systems have been used to mimic DCs, also referred to as artificial antigen presenting cells (aAPCs).[15] Cellular aAPCs have been made from human leukemia or melanoma cell lines, insect cells, and mouse fibroblasts. However, these systems require genetic modifications to effectively present antigens and represent an allogenic component in the cell culture and final cell product (reviewed in a study conducted by Hasan *et al*[14]). Among acellular aAPCs, commercial microbeads with activating antibodies towards CD3 and CD28 are the most commonly used and clinically relevant.[16] Despite their wide use, the rigid beads fail to fully replicate the complex properties of APCs, resulting in suboptimal expansion rates and dysregulated T-cell functions.[17–19] In addition, the beads require removal prior to clinical use, providing additional stress and handling of the T-cell product. The same holds true for the more recently developed paramagnetic nanoparticle-based aAPCs.[20 21] To overcome above-mentioned challenges, a number of biomaterial-based aAPCs have been developed over the past years, however, many represent rather complex structures, and most do not offer a pMHC-TCR-driven interaction with antigen-specific T-cells (reviewed in a study conducted by Isser *et al*[22]).

Taken together, we demonstrate a novel clinically applicable technology for the expansion of both virus-specific and tumor antigen-specific T-cells ex vivo. Using Ag-scaffolds, endogenous antigen-specific T-cells can be expanded from peripheral blood to obtain a T-cell product with a phenotypic and functional profile that is favorable for ACT.

MATERIALS AND METHODS

Samples and cell lines

PBMCs from healthy donors were isolated from buffy coats, available from the Central Blood Bank of the Copenhagen University Hospital (Rigshospitalet) and were purified by density centrifugation using Lymphoprep (Axis-Shield PoC). PBMCs or tumor fragment/digest from patients with metastatic melanoma were obtained from the National Center for Cancer Immune Therapy (CCIT-DK) at Herlev University Hospital, Denmark. Patients in cohort 1 (MM1, n=9) were treated with checkpoint inhibitors at the Department of Oncology at Herlev Hospital and enrolled in a non-interventional biomarker study registered at the Capital Region Ethics Committee (H-15007985). Patients in cohort 2 (MM2, n=10) were enrolled in a trial of combination therapy with nivolumab and PD-L1/IDO peptide vaccine (NCT03047928). HLA-A0201-negative FM45 (ESTDAB-011) and HLA-A0201-positive FM3 (ESTDAB-007) and FM93/2 (ESTDAB-033) melanoma tumor cell lines were purchased from the European Searchable Tumor Cell Line Database (ESTDAB) (online supplemental table 1).[23] HLA-A0201-positive T2 lymphoblast cells (CRL-1992) were purchased from American Type Culture Collection (ATCC). All samples were cryopreserved in fetal calf serum (FCS) with 10% Dimethyl sulfoxide (DMSO) and stored in liquid N_2 until use.

pMHC and tetramer generation

Peptides were purchased from Pepscan (Pepscan Presto BV) and dissolved to 10 mM in DMSO. Recombinant Human Leukocyte Antigen (HLA) heavy chains and human β2 microglobulin light chain were produced in *Escherichia coli*. For HLA-A0101, HLA-A0301 and HLA-B0702, heavy and light chains were refolded with ultraviolet (UV)-sensitive ligands and purified as previously described.[24] pMHC complexes were generated by UV-mediated exchange.[25] For HLA-A0201, we used a functionally empty disulfide-stabilized variant which is peptide-receptive and can be loaded by incubation with peptide for 15 min at room temperature.[26] Exchanged pMHCs were centrifuged for 5 min at 3300 g to exclude unwanted aggregates.

Tetramers were generated by adding 9.02 uL (online supplemental table 1, Stock concentration 0.2 mg/mL) or 18.04 uL (online supplemental table 1, Stock conc. 0.1 mg/mL) streptavidin fluorochrome conjugate per 100 uL of pMHC monomers (100 ug/mL) and incubating for 30 min at 4°C, followed by addition of D-Biotin (Avidity, BIO-200) at a final concentration of 25 uM to block any free binding sites.

PBMCs from healthy donors and patients with metastatic melanoma were screened for T-cell recognition of virus or cancer epitopes, respectively, using combinatorial encoded tetramers[27 28] or DNA-barcoded pMHC multimers.[29]

Ag-scaffold generation

Ag-scaffolds were assembled, using a streptavidin-conjugated dextran backbone (500 kDa) (Fina Biosolutions) mixed with biotinylated MHC class I molecules holding a given peptide, and biotinylated co-stimulatory molecules (B7.2/CD86-mulg-biotin, Mybiosource.com MBS666812) and/or cytokines (IL-15, Peprotech 200–15, IL-2 Avitag, Acro IL-2H82F3, IL-21 Avitag, Acro IL-21-H82F7), followed by incubation at 4°C for 30 min. Ag-scaffolds were incubated with D-Biotin at 4°C for 20 min to block potential free streptavidin-sites on the dextran backbone. To remove any unbound molecules, Ag-scaffolds were filtered through 100 kDa spin columns (Vivaspin6, Sartorius). Ag-scaffold were stored in a humid chamber at 4°C during the 2-week expansion or supplemented with 10× Freeze Buffer (5% Bovine Serum Albumin (BSA)+50% Glycerol) and stored at −80°C up to 15 months.

Antigen-specific T-cell expansion

Pre-existing T-cell responses were expanded from PBMCs, by culturing them for 2 weeks in X-VIVO 15 media (Lonza, BE02-060Q) supplemented with 5% human serum (Sigma Aldrich Heat Inactivated H3667) and Ag-scaffold (0.16 nM prefiltration) or specific peptide (5 µM), soluble IL-2 (40 U/mL, Peprotech 200–02) and soluble IL-21 (25 ng/mL, Peprotech 200–21). Ag-scaffold or free components were added on culture initiation and two times per week until harvest.

T-cell staining and flow cytometry

Antigen-specific T-cell populations were stained by incubation with R-phycoerythrin (PE)-labeled or Fluorescein isothiocyanate (FITC)-labeled dextran backbone (Fina Biosolutions) or tetramer for 15 min at 37°C, followed by staining for live cells (LIVE/DEAD Fixable Near-IR, Invitrogen 2451278) and surface markers CD3 and CD8 (online supplemental table 2) at 4°C for 30 min. For further characterization of the antigen-specific T-cell population, an antibody panel was included in the surface marker staining (online supplemental table 2). Stained samples were analyzed on a Fortessa LSR flow cytometer (BD) and data analysis was carried out using the FlowJo V.10 software. The multidimensional analysis, including uniform manifold approximation and projection illustration and FlowSOM unsupervised clustering analysis, was performed within the FlowJo application.

Intracellular cytokine staining

Expanded T-cells were incubated with peptide-pulsed T2 target cells (E:T 1:1) for 4–10 hours in X-VIVO 15 media supplemented with αCD107a-PE antibody (online supplemental table 1) and GolgiPlug (BD Bioscience, 550583). A negative and positive control was incubated with non-pulsed T2 cells and leukocyte activating cocktail (LAC, Vendor, 550583), respectively. Harvested T-cells were stained for dead cells and surface markers (αCD3-FITC and αCD8-BV480, online supplemental table 2) as described above, fixed and permeabilized (Invitrogen, 88-8824-00) and stained for intracellular markers

(TNFα-PE-Cy7 and IFNγ-APC, online supplemental table 1) at 4°C for 30 min followed by flow cytometry analysis.

Single-cell transcriptomic and phenotypic analysis

Expanded T-cells were incubated 1 hour at 4°C with PE/APC tetramers for staining of the relevant antigen-specific T-cells. Subsequently, cells were washed three times in phosphate buffered saline (PBS)+0.5% BSA and stained with the TotalSeq-C Human Universal Cocktail (BioLegend # 399905) phenotype panel and individual TotalSeq-C0251 (BioLegend # 394661) hashing antibodies according to manufactures' instructions. After 15 min incubation at 4°C, cells were co-stained with CD8-BV480 and dump channel antibodies (online supplemental table 1) and a dead cell marker and incubated 30 min, 4°C. Cells were washed three times through sedimentation at 390 g and resuspended in PBS+0.5% BSA before sorting single, live, $CD8^+$ and tetramer positive cells on a BD FACS Melody cell sorter. Tetramer-positive T-cells (n=2500) from each sample were sorted into a common tube and centrifuged on 390 g for 10 min at 4°C. The supernatant was removed, and cells were loaded onto Chromium according to the manufacturer's instructions. We used the 10×5' v2 chemistry that allows the cell barcode to be appended at the 5'-end of transcripts, which is essential for capturing the CDR3 region of the V(D)J transcripts. Downstream processing of messenger RNA (mRNA) and DNA barcodes are performed according to manufacturer's instructions (Chromium Next GEM Single Cell 5' Reagent Kits v2 (Dual Index), with the Feature Barcode technology for Cell Surface Protein & Immune Receptor Mapping) (10x Genomics, USA). Overall, ~13 750 cells were loaded (based on 55% recovery from 25,000 sorted cells) to yield a maximum of 8,000 cells with an intermediate/high doublet rate (6.9%). Targeted amplification was performed for 13 cycles and the products were separated according to size into <400 bp (DNA barcode-tags) and >400 bp (the TCR sequences) using 0.6× SPRIselect beads (Beckman Coulter, B23318). Separate processing of the >400 bp bead-bound TCR sequences and the <400 bp in solution DNA barcodes was conducted according to manufacturer's instruction and the TCR amplification products were sequenced on a NovaSeq running a 150 paired-end program. DNA barcodes, TCR sequences and mRNA were sequenced to a depth of 6,181, 6,598 and 32,136 mean reads per cell, respectively.

The raw FASTQ files were processed using the CellRanger multi pipeline (10x Genomics, V.6.1.1) and the filtered gene-barcode matrices were used for further analysis using the R software (V.4.1.0) with the Seurat package (V.4.1.0). Following filtration, a total of 2,649 cells; 1,832 cells for donor BC-349 (209 unexpanded, 773 Free peptide-expanded, and 850 Ag-scaffold-expanded T cells) and 817 cells for donor BC-357 (350 unexpanded, 66 Free peptide-expanded and 401 Ag-scaffold-expanded T-cells) were included in further analyses. For the TCR analysis we used the filtered TCR diversity metric and only cells with at least one productive TCR α-chain and one productive TCR β-chain were kept for further analysis. Cell Hashing was used to place a sample barcode on each single cell, enabling different samples to be multiplexed together and run in a single experiment. To demultiplex the samples the HTODemux (positive.quantile=0.99) from Seurat was used and only cells labeled as Singlets were used.

For the gene expression analysis, only genes detected in >3 cells and cells with >200 detected genes were selected. Low-quality cells were removed if they had: (1) <6,000 genes detected in each cell, (2) <25,000 molecules detected within a cell, and (3) >5% Unique Molecular Identifiers (UMIs) derived from the mitochondrial genome. After the removal of low-quality cells, gene expression matrices were normalized using the SCTransform function and the effect of the cell cycle was removed by regressing out the S scores and G2/M scores during data scaling. The cell surface protein analysis was performed with cell surface proteins from the TotalSeq-C library, and the phenotype data were normalized using the SCTransform function.

For differential expression analysis, we used the FindAllMarkers function to identify positive markers of each group and compared this to all other cells from the remaining groups (online supplemental figure 3). For comparing T-cells expanded using Ag-scaffold and free peptide, we used the FindMarkers function. Heatmaps were generated using the DoHeatmap function from Seurat and volcano plots were generated using EnhancedVolcano V.1.10.0. The gene set enrichment analysis was performed with enrichplot V.1.12.3 and clusterProfiler V.4.0.5, using Benjamini-Hochberg for adjusting p values.[30]

The dysfunctional score for each Gel Bead-in Emulsions (GEM) was calculated as the mean expression of a set of dysfunctional genes identified by Li *et al*. Only 23 out of the original 30 published dysfunctional genes were included in our data set, since 7 genes were not among the top 2000 most differentially expressed genes according to SCTransform.[31]

moDC-mediated expansion of antigen-specific T-cells

Monocyte-derived dendritic cells (moDC) were generated from autologous PBMCs using Dendritic Cell Generation media (PromoCell) according to manufacturer's instructions. Briefly, adherent cells, including monocytes, were first enriched from PBMCs by incubation in Monocyte attachment media (PromoCell). The enriched cells were next incubated in dendritic cell generation media supplemented with component A. After 6 days (with media change halfway), cultures were supplemented with component B, and the cells incubated for another 24–48 hours, whereafter mature moDCs were collected after washing. Mature moDCs were pulsed with the specific peptide for 2 hours at room temperature. Autologous specific T-cells were expanded from PBMCs by culturing for 10 days with peptide-pulsed moDCs at a 1:10 ratio (500,000 moDCs to 5,000,000 PBMCs) in X-vivo

supplemented with 5% human serum, with addition of new peptide-pulsed moDCs after 5 days of culture.

Tumor cell killing

FM3, FM93/2 and FM45 melanoma cells were seeded at a density of 20,000 cells/well in preheated RPMI-1640 media with 10% FCS into an E-plate 96 PET (Agilent 300600900).[32] Post-seeding, the E-plate was transferred to an xCELLigence RTCA SP or eSight instrument (Agilent) inside a cell incubator and incubated for 24 hours. Data recording was set to 1 hour intervals over 72 hours and changes in impedance were reported as a Cell Index (CI). After 24 hours, tumor cell CI was set to 1 and expanded T-cells were added to the tumor cell cultures with an effector:target ratio of 4:1. Negative control wells contained tumor cells alone and positive control wells were treated with Triton X-100. Tumor and expanded T-cells were co-cultured for another 48 hours. The CI at each time point was normalized to CI_{Triton} and expressed as the percentage of survival compared with tumor alone.

Bulk TCR sequencing

Expanded T cells were incubated 15 min at 37°C with PE/APC tetramers for staining of the relevant antigen-specific T cells followed by staining with surface markers (αCD3-FITC and αCD8-BV480) and a dead cell marker for 30 min at 4°C. Tetramer-positive $CD8^+$ T-cells were sorted into PBS+2% FCS + 0.025M HEPES buffer on a BD FACS Melody cell sorter and centrifuged at 390 g for 10 min and the supernatant was removed. Pellets were snap frozen and sent for DNA purification and TCR β-chain sequencing using the ImmunoSEQ platform at Adaptive Biotechnologies.

Statistical analysis

The sample size for all experiments were chosen on the basis of sample availability and what was sufficient for statistical analysis. All statistical analyses were performed using the GraphPad Prism 7 software. All data are presented as individual data points including grand median or as means±SD. Technical replicates were averaged and treatment groups were compared using a paired or unpaired, non-parametric Wilcoxon or Mann-Whitney test, respectively, as indicated in figure legends.

RESULTS

Ag-scaffold-based expansion is pMHC-dependent

Ag-scaffolds are designed to ensure pMHC-directed expansion of specific T-cells, while avoiding unspecific expansion of bystander T-cells. Therefore, it is critical that the Ag-scaffold interaction with T-cells is mediated by attached pMHC elements. First step in designing a specific Ag-scaffold is to determine the amount of pMHC molecules required on the dextran backbone to ensure specific pMHC-TCR-driven binding to T-cells. pMHC (cytomegalovirus (CMV) 65kDa phosphoprotein (pp65) YSE-peptide on HLA-A0101) was titrated onto fluorescently-labeled dextran, to evaluate binding to $CD8^+$ T-cells from healthy donor PBMCs with a known T-cell response against this peptide (~4% of CD8 T-cells). Based on mean fluorescence intensity (MFI) of the Ag-scaffold-binding population and Staining Index (SI), we demonstrated optimal T-cell binding using a molar ratio of approximately 10 pMHC molecules per dextran backbone (figure 1A,B). Similarly, we determined the amount of co-stimulatory molecules and cytokines that could be co-attached to the 1:10 Dex:pMHC without compromising the pMHC-TCR interaction, using the CD28-ligand B7.2 and IL-15. We thereby identified an optimal molar ratio for a Dex:pMHC:B7.2:IL-15 Ag-scaffold (1:10:5:5) (figure 1C). The optimal ratio for a given Ag-scaffold, depends on the dextran backbone and co-attached pMHCs and stimulatory molecules and should ideally be determined for every new composition (online supplemental figure 1A,B). The optimal ratio for Ag-scaffolds not carrying a fluorescent label can be determined based on expansion capacity (online supplemental figure 1C).

To show that the interaction between the Dex:pMHC:B7.2:IL-15 Ag-scaffold and specific T-cells was in fact directed by the pMHCs and not the co-stimulatory molecules nor cytokines, Ag-scaffolds comprizing only dextran and B7.2 or IL-15 failed to bind the specific T-cells (figure 1D). Finally, using the 1:10:5:5 Dex:pMHC:B7.2:IL-15 Ag-scaffold, we expanded a population of HLA-A0101-restricted Influenza polymerase basic protein (BP) VSD-specific $CD8^+$ T-cells from PBMCs from healthy donor PBMCs (precursor frequency~0.1%). During the expansion-process, Ag-scaffold and fresh media was provided to the culture four times, on days 0, 3, 7 and 10 (figure 1E). After 2 weeks, the population of Influenza BP VSD-specific T-cells had expanded to 6.3%, while no expansion was observed when providing a similar Ag-scaffold with an irrelevant pMHC (figure 1F). In addition, only limited bystander expansion of a predetected population of HLA-A0201 Influenza M1 58–66-specific CD8+T cells (~0.2%) was observed, during Ag-scaffold-directed expansion of HLA-A0201 CMV BRLF1-specific T-cells (online supplemental figure 1F).

To show that multiple antigen-specific T-cells can be expanded simultaneously from a single culture by adding a mix of Ag-scaffolds, each containing different pMHCs, we expanded CMV pp65 NLV-specific and Epstein-Barr virus (EBV) latent membrane protein 2 (LMP2) FLY-specific T-cells from healthy donor PBMCs, using a pool of 10 Ag-scaffolds including only one carrying a relevant pMHC. The expansion capacity of a relevant Ag-scaffold, was not affected by the presence of nine irrelevant Ag-scaffolds (online supplemental figure 2A). Similarly, five antigen-specific T-cells populations could be expanded in a single culture using a mix of 5 relevant and 25 irrelevant Ag-scaffolds. The resulting T-cell product was composed of 66.3% antigen-specific T-cells, compared with 0.23% prior to expansion (online supplemental figure 2B,C).

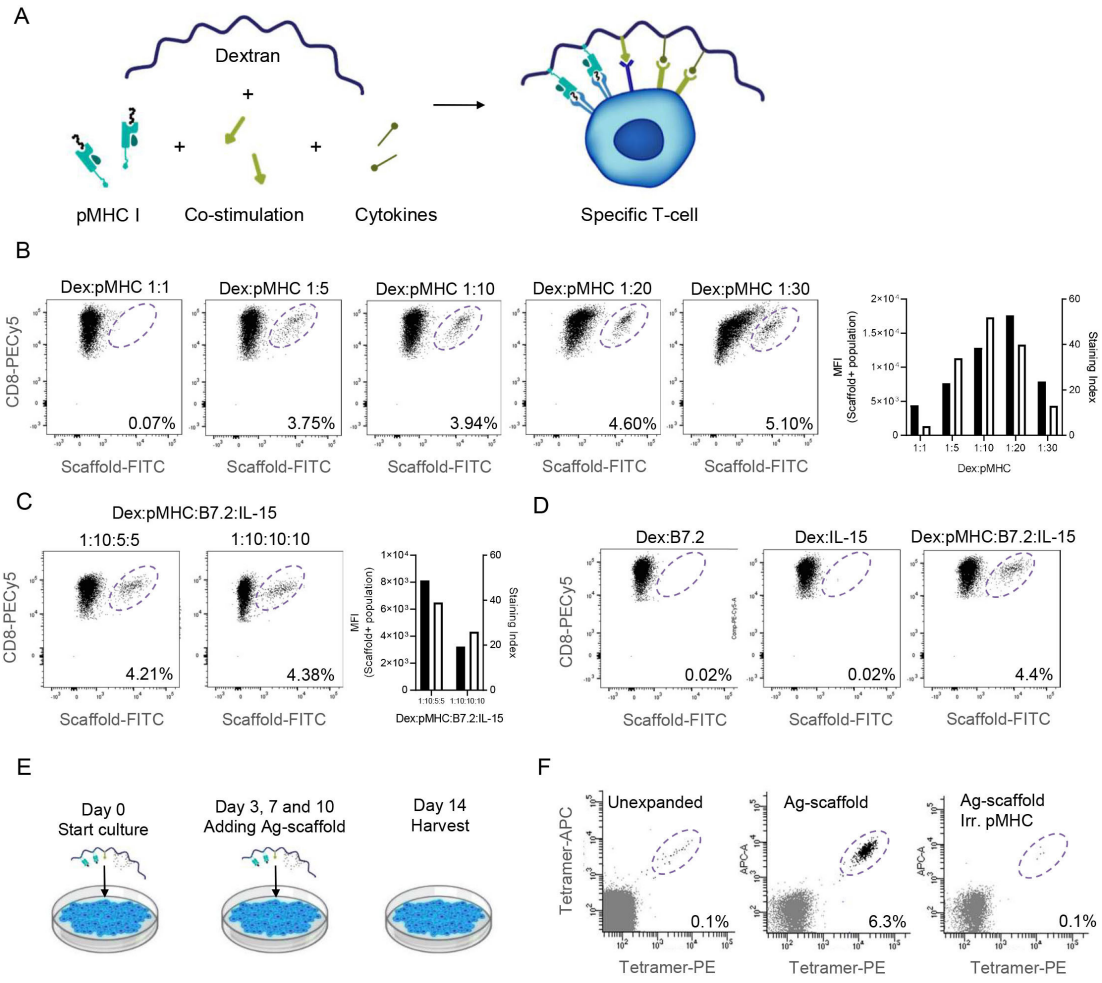

Figure 1 Ag-scaffolds bind to specific T-cells via attached pMHC I and delivers co-attached co-stimulation and cytokines. (A) Schematic drawing of an Ag-scaffold comprizing a dextran backbone to which MHC class I molecules carrying peptide (pMHC), co-stimulatory molecules and cytokines can be attached. The Ag-scaffold bind to T-cells via pMHC-TCR-interaction and forms an artificial immunological synapse. (B) Binding of FITC-labeled dextran-backbone with varying amounts of pMHCs, to HLA-A0101 CMV pp65 YSE-specific T-cells (~4%). Ratios were compared in median fluorescent intensity (MFI in black) and staining index (SI in white). $CD8^+$ T-cells were labeled with PECy5. (C) T-cell binding of a 1:10 dextran:pMHC in combination with either 5:5 or 10:10 of B7.2:IL-15. (D) Ag-scaffolds comprizing only dextran:B7.2 (1:30) or dextran:IL-15 (1:30) could not direct T-cell binding. (E) Schematic representation of a 2 week Ag-expansion where Ag-scaffold and fresh media is supplemented to the culture on day 0, 3, 7 and 10. (F) Only Ag-scaffolds (dextran:pMHC:B7.2:IL-15) containing HLA-A0101 carrying the Influenza BP VSD-peptide and not an irrelevant pMHC, could expand a population of HLA-A0101 Influenza BP VSD-specific T-cells from PBMCs from a healthy donor. Specific cells were stained with a PE/APC-tetramer. Ag-scaffolds, antigen-presenting scaffold; APC, Allophycocyanin; BP, polymerase basic protein, CMV, cytomegalovirus, dex, dextran; FITC, Fluorescein isothiocyanate; HLA, human leukocyte antigen; IL, interleukin; MHC, Major Histocompatibility Complex; PBMCs, peripheral blood mononuclear cells; PE, R-phycoerythrin; TCR, T-cell receptor; VSD, the first three aminoacids of the peptide.

Taken together, this demonstrates that Ag-scaffolds are capable of binding antigen-specific T-cells via pMHC-TCR interaction and drive their selective expansion from low precursor numbers in a mixture of irrelevant lymphocytes, by delivering co-stimulatory and growth signals. This allows expansion of multiple antigen-specific T-cell populations, simultaneously in a single culture using a mix of Ag-scaffolds.

An Ag-scaffold with IL-2 and IL-21 is superior in expansion-efficiency and expanded T-cell functionality

The Ag-scaffold technology is highly flexible; it only requires a site-directed biotinylation of a molecule of choice and attachment to the streptavidin-decorated dextran backbone. Thus, an endless variety of Ag-scaffolds can be designed to support many different biological needs. In order to identify an optimal combination of cytokines and co-stimulation for expansion of antigen-specific T-cells for ACT, we assembled 66 individual Ag-scaffolds, using different combinations of cytokines and co-stimulatory molecules and compared them in terms of expansion efficiency (frequency of antigen-specific T-cells post expansion) and the functional capacity of expanded T-cells. For all Ag-scaffold compositions not containing IL-2, low concentrations of IL-2 (40 U/mL) was supplemented to the culture media. The frequency of

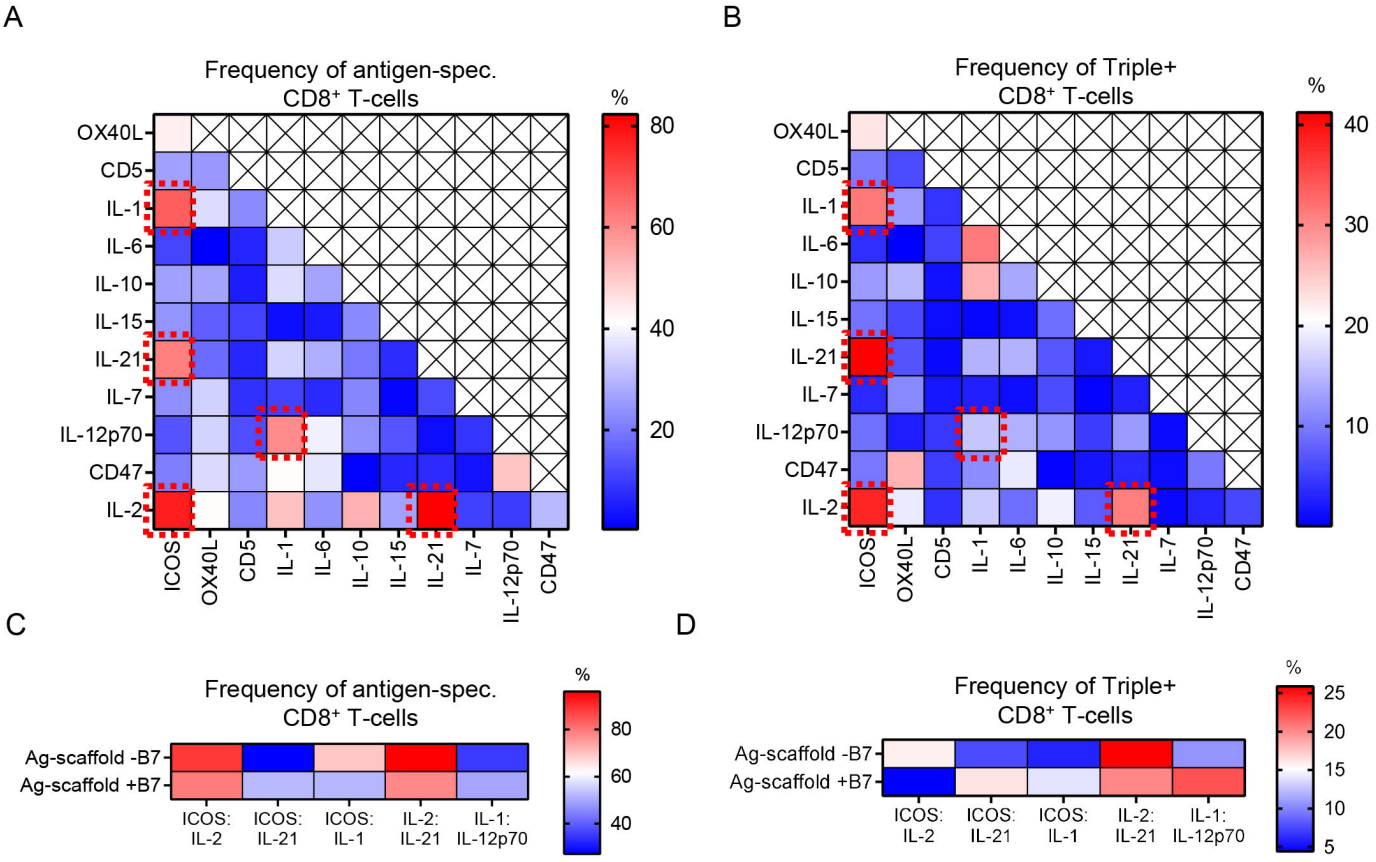

Figure 2 An Ag-scaffold with IL-2 and IL-21 is superior in terms of expansion capacity and functionality of expanded cells. (A) Frequency of HLA-A0201 EBV BRLF1 YVL-specific CD8+ T-cells from PBMCs from one healthy donor after a 2-week expansion with 66 different dextran:pMHC:molecule 1:molecule 2 Ag-scaffold-combinations. (B) Frequency of T-cells with simultaneous expression of IFN-γ, TNF-α and CD107a (Triple+T cells) out of the total CD8+ T-cell population on antigen-challenge. IL-2 (40 U/mL) was supplemented to the media in cultures expanded with Ag-scaffold not containing IL-2. The best performing five Ag-scaffold combinations were marked in dashed red boxes. (C) Frequency of HLA-A0101 CMV pp50 VTE-specific CD8+ T-cells from PBMCs from one healthy donor after a 2-week expansion with the five selected combinations in a dextran:pMHC:molecule 1:molecule 2 (Ag-scaffold –B7) or a dextran:pMHC:B7.2:molecule 1:molecule 2 (Ag-scaffold+B7). (D) Frequency of Triple+ (IFN-γ+TNF-α+CD107a+) T-cells out of the total CD8+ T-cell population on antigen-challenge. Red and blue scaling represent the highest and lowest frequency of CD8+ T-cells, respectively. Ag-scaffolds, antigen-presenting scaffold; EBV, Epstein-Barr virus; HLA, human leukocyte antigen; ICOS, Inducible T-cell COStimulator; IFN, interferon; IL, interleukin; MHC, major histocompatibility complex; PBMCs, peripheral blood mononuclear cells; pp50, 50kDa phosphoprotein, pMHC, peptide-MHC; TNF, tumor necrosis factor.

antigen-specific T-cells out of CD8+ T cells was evaluated for all Ag-scaffold compositions (figure 2A, online supplemental table 3). We further evaluated the functional potential of expanded T-cells using intracellular cytokine staining on co-culture with target cells pulsed with cognate antigen and defined it as the frequency of T-cells expressing a combination of pro-inflammatory cytokines tumor necrosis factor (TNF)α, interferon (IFN)γ and CD107a, a marker of degranulation[33 34] (figure 2B). Using this matrix-based approach, we identified several novel Ag-scaffold compositions with capacity to drive antigen-specific T-cell expansion and produce multifunctional T-cells. We selected the five compositions (Inducible T-cell COStimulator (ICOS:IL-2, ICOS:IL-21, ICOS:IL-1, IL-2:IL-21, IL-1:IL-12) that demonstrated the strongest T-cell expansion capacity, while also providing a good functional profile (figure 2A,B).

We further evaluated the performance of the top-five Ag-scaffold compositions, either with or without addition of a B7.2 co-stimulatory molecule (figure 2C,D, online supplemental table 3). While no further benefit was gained from the addition of B7.2 co-stimulation to the Ag-scaffold in the current setting, Ag-scaffolds with ICOS:IL-2 and IL-2:IL-21 were superior when comparing post-expansion frequency of antigen-specific T-cells (figure 2C). Considering the functional capacity of expanded T-cells, the Ag-scaffold with IL-2 and IL-21 demonstrated superior properties (figure 2D). This scaffold design has the further advantage that no soluble cytokines were added to the media, reducing the level of bystander T-cell stimulation in the culture. In the following analyses presented here, we will focus on the selected Dex:pMHC:IL-2:IL21 Ag-scaffold.

Evaluation of the wide range of Ag-scaffold compositions demonstrates the flexibility of the Ag-scaffold technology and introduces several functional Ag-scaffold combinations that can be of potential interest in various immunological settings. For the purpose of generating antigen-specific T-cell products for ACT, the Ag-scaffold with IL-2 and IL-21 showed the greatest expansion efficiency and production of multifunctional T-cells, which is desired for such setting.

Ag-scaffolds efficiently expand virus-specific T-cells and render a multifunctional T-cell product

To further evaluate the capacity of Ag-scaffold-directed T-cell expansion, the expansion efficiency and functional profile of expanded T-cells was compared with free peptide-based expansion, in which all components attached to the Ag-scaffold was added to the T-cell culture in a non-orchestrated manner, that is, soluble specific peptide co-administered with soluble IL-2 and IL-21. The two strategies were compared across a total of 15 virus-specific T-cell populations in PBMCs from 11 healthy donors. During expansion, Ag-scaffold or soluble peptide and cytokines were supplemented to the culture media at initiation (day 0) and two times per week (days 3, 7 and 10) until harvest. While no difference between free peptide-based and Ag-scaffold-expansion was observed in terms of total viable cell count on harvest, Ag-scaffold-directed expansion yields both a higher frequency and absolute number of antigen-specific T-cells (figure 3A–C).

In order to compare the phenotype of T-cells expanded with either Ag-scaffold or free peptide, we stained the antigen-specific population with a panel of T-cell markers covering different stages of $CD8^+$ T-cell differentiation. Clustering analysis of free peptide based and Ag-scaffold-expanded CMV pp50 VTE-specific T cells in two healthy donors showed that the two strategies yield very different T-cells products. Ag-scaffold-expanded T-cells expressed higher levels of TCF1, a transcription factor typically expressed by previously activated $CD8^+$ T-cells with self-renewal capacity, and co-stimulatory and early effector-memory markers CD27 and CD28, and lower levels of markers associated with terminal differentiation and exhaustion; Thymocyte selection-associated high mobility group box protein (Tox), Programmed cell death protein 1 (PD-1) and granzyme B (GzmB), when comparing with free peptide-expanded T-cells (figure 3D, online supplemental figure 3A). This was further supported when comparing both the expression level (MFI) of the individual markers and their combined expression on expanded T cells, in a total of four different virus-specific T-cell populations expanded in duplicate from four healthy donors (figure 3E,F), suggesting that Ag-scaffold-expanded T-cells are less exhausted and maintain stem-like features. In addition, the phenotypic characteristics of Ag-scaffold-expanded T-cells were compared with antigen-specific T-cells expanded with peptide-pulsed autologous moDCs. The moDC-expanded and Ag-scaffold-expanded T-cells demonstrated very similar phenotypic characteristics, while moDC-directed expansion seemed to provide a higher number of antigen-specific T-cells (online supplemental figure 3B).

In accordance with observed differences between Ag-scaffold-directed and free peptide-directed expansion in terms of frequency and phenotype of antigen-specific T-cells, Ag-scaffold-expanded T-cells had a higher frequency of cytokine-producing T-cells (triple-positive, double-positive and single-positive for TNFα, IFNγ and CD107a) of $CD8^+$ T-cells when challenged with cognate antigen (figure 3G).

Single-cell transcriptomic and phenotypic analysis of unexpanded, free peptide-expanded or Ag-scaffold-expanded HLA-A0301 Influenza NP IRL-specific and HLA-B0702 CMV pp65 TPR-specific T cells from two healthy donors further elucidated differences between the resulting T-cell products (figure 3H, online supplemental figure 3C–E). On the transcriptional level, Ag-scaffold-expanded T-cells showed a higher expression of genes linked with transitional and cytotoxic effector T-cells (GZMH/K, FGFBP2, KLF2),[35] TCR signaling (IFITM1/2, GIMAP4/7, TRAV17, TRAB7-9, LIME1)[36–38] and T-cell survival (KLF2, BATF)[39] compared with free peptide-expanded T-cells. Conversely, Ag-scaffold-expanded T-cells had a lower expression of genes that have been linked with T-cell dysfunction (ENTPD1, CCL3/4, FAM3C, TSC22D3),[35 40] activation-induced cell death (PHLDA)[41] and T-cell signal transduction (MAL, SLC1A5) (online supplemental figure 3C,D). On the phenotypic level, Ag-scaffold-expanded T-cells again showed a higher expression of CD27 and CD28, along with proteins associated with central T-cell memory (CD62L), late stage effector phenotype (CD16, CD5, KLGR1)[42] and antigen-experience (CD49d, CD244, Fas)[43 44] and a lower expression of proteins associated with terminal differentiation/activation-induced cell death (CD25)[45 46] and exhaustion (CD39)[8 47] when compared with free peptide-expanded T-cells (figure 3H, online supplemental figure 3E). Accordingly, free peptide-expanded T-cells showed higher activity of a recently described dysfunctional gene module (dysfunctional score) compared with unexpanded and Ag-scaffold-expanded T-cells (figure 3I).[31] When evaluated individually, most of the genes included in the dysfunctional score were expressed at a higher level in free peptide-expanded T-cells, compared with Ag-scaffold-expanded T-cells (online supplemental figure 3F). Finally, single-cell TCR sequencing showed that Ag-scaffold-expanded and free peptide-expanded HLA-A0301 Influenza NP IRL-specific and HLA-B0702 CMV pp65 TPR-specific T-cell populations from healthy donors BC349 and BC357, respectively, comprised of multiple TCR clones and that the selection of TCR clones between the two expansion strategies was very similar (online supplemental figure 3G)

This shows that Ag-scaffold-directed expansion yields a greater frequency of virus-specific T-cells, with a younger phenotype and greater cytotoxic potential on

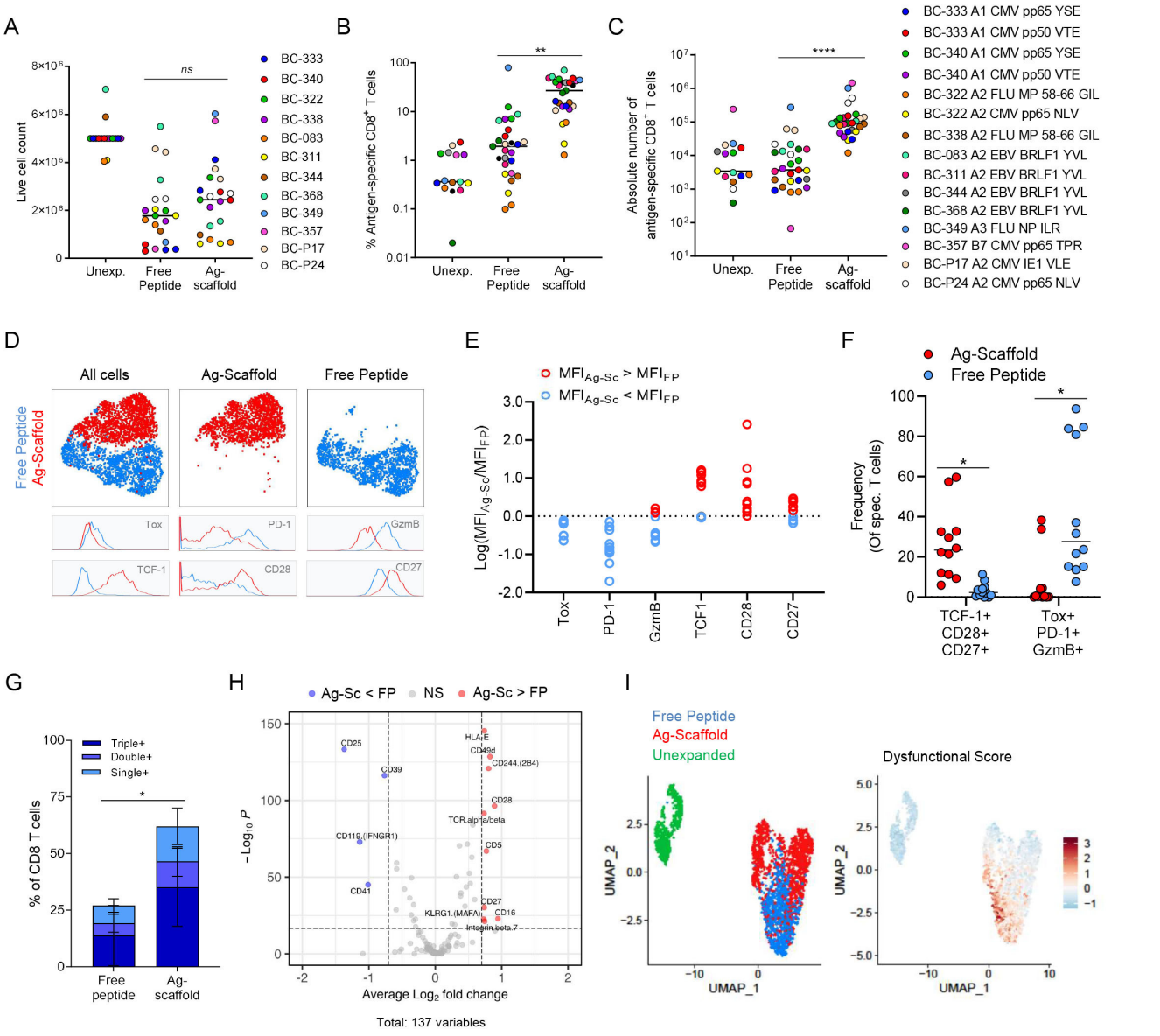

Figure 3 Ag-scaffolds efficiently expand virus-specific T-cells and render a multifunctional T-cell product. (A) Number of viable cells at culture initiation (Unexp.) and following 2-week expansion with either dextran:pMHC:IL-2:IL:21 Ag-scaffold or free peptide-based expansion, adding specific peptide, IL-2 and IL-21 directly to the media, across 12 healthy donors in duplicate cultures. (B) Post-expansion frequency and (C) number of virus-specific T-cells from 15 parallel expansions in duplicate, covering 9 different virus-specific T-cell populations in PBMCs from 12 healthy donor buffycoats (BC), with either Ag-scaffold or free peptide-based expansion. (D) UMAP plot of HLA-A0101 CMV p50 VTE-specific T-cells expanded in duplicate from two healthy donors with either Ag-scaffold or free peptide. Specific T-cells were identified by tetramer-staining and stained with an antibody panel including markers of self-renewing (TCF-1, CD28, CD27) and terminally differentiated/exhausted (Tox, PD-1, GzmB) T-cells. The expression of these markers on Ag-scaffold (red) and free peptide (blue)-expanded T-cells were compared in MFI histograms. (E) Broadened phenotypic comparison between Ag-scaffold and free peptide-expanded T-cells ($Log(MFI_{Ag\text{-}Sc}/MFI_{FP})$) across four different virus-specific T-cell populations expanded in duplicate from four healthy donors. (F) Frequency of $TCF\text{-}1^{+}CD28^{+}CD27^{+}$ and $PD\text{-}1^{+}GzmB^{+}Tox^{+}$ T-cells out of antigen-specific T-cells expanded with either Ag-scaffold and free peptide. (G) Frequency of Triple+, Double+ and Single+ for IFN-γ, TNF-α and CD107a+ out of the total CD8+T-cell population on challenge with cognate antigen in expansions of HLA-A0201 CMVpp65 NLV-specific and EBV BRLF1 YVL-specific T-cells from eight healthy donors. (H) Single-cell phenotypic analysis and (I) dysfunctional score in a UMAP plot of unexpanded or free peptide-expanded and Ag-scaffold-expanded HLA-A0301 Influenza NP IRL-specific and HLA-B0702 CMV pp65 TPR-specific T cells from two healthy donor BCs, respectively. Duplicate-means were compared in a paired, non-parametric Wilcoxon test and $p<0.05$, $p<0.01$, $p<0.0001$ is indicated as *, ** and ****, respectively. Ag-scaffolds, antigen-presenting scaffold; BCs, buffycoats; CMV, cytomegalovirus; EBV, Epstein-Barr virus; GzmB, granzyme B; HLA, human leukocyte antigen; IL, interleukin; IFN, Interferron; MFI, mean fluorescence intensity; NLV, first three amino acids of peptide; PBMCs, peripheral blood mononuclear cells; pMHC, peptide-MHC; PD-1, Programmed cell death protein 1;TCF, transcription factor T-cell factor 1; TNF, tumor necrosis factor; Tox, Thymocyte selection-associated high mobility group box protein; UMAP, uniform manifold approximation and projection; VTE, first three amino acids of peptide

antigen-challenge, when compared to conventional expansion with free peptide and cytokines.

Ag-scaffolds expand tumor-specific T-cells from patient with cancer PBMCs

The Ag-scaffold technology presents a potential improvement to the T-cell expansion step preceding ACT in anticancer immunotherapy. We therefore investigated the capacity of Ag-scaffolds to expand tumor-specific T-cells from PBMCs from patients with metastatic melanoma. In six patient samples (MM1.06 and MM1.32, evaluation 3 and 5 and MM1.12 and MM1.29, evaluation 3), we compared Ag-scaffold-directed and free peptide-directed expansion of a total of seven previously observed responses against HLA-A0201-restricted tumor shared antigens (TSAs). Consistent with our observation when expanding virus-specific $CD8^+$ T-cells from healthy donors, Ag-scaffold-directed expansion yielded a greater number of viable cells and antigen-specific T cells compared with free peptide-directed expansion (figure 4A–C).

Clustering analysis of free peptide-expanded and Ag-scaffold-expanded gp100/Pmel17 YLE-specific T-cells from one patient with metastatic melanoma, similarly showed that Ag-scaffold-expanded and free peptide-expanded tumor-specific T-cells were phenotypically distinct (figure 4D, online supplemental figure 4A). When comparing the expression of individual markers of terminal differentiation/exhaustion and self-renewal on expanded tumor-specific T-cell populations (gp100/Pmel17 YLE and KTW) from four patient PBMC samples, along with the frequency of cells expressing a combination of these markers, we observed more self-renewal characteristics in the populations expanded with Ag-scaffolds (figure 4E,F).

To further evaluate the functional capacity of Ag-scaffold-expanded T-cells, Ag-scaffold or free peptide-expanded tumor-specific T-cells from patient MM1.06-E3 and MM1.32-E3 were co-cultured for 48 hours with HLA-A0201-positive FM3 and FM93/2 melanoma cells. FM3 and FM93/2 express a range of shared melanoma antigens, including those used for antigen-directed T-cell expansion (online supplemental table 2).[23 48] The Ag-scaffold-expanded and free peptide-expanded T-cell products from MM1.06-E3, consisted of 12.7 and 7.15% Gp100/Pmel17 YLE-specific T-cells, 18.4 and 33.9% Gp100/Pmel17 KTW-specific T-cells and 1.18 and 0.5% Melan-A/MART-1 EEA-specific T-cells, respectively (figure 4B), while the Ag-scaffold-expanded and free peptide-expanded T-cell products from MM1.32-E3 consisted of 42.6 and 29.6% Gp100/Pmel17 IMD-specific T-cells and 7.7 and 11.9% Gp100/Pmel17 KTW-specific T-cells, respectively (figure 4B). Ag-scaffold-expanded T-cells from both MM1.06-E3 and MM1.32-E3 exhibited a higher level of killing of both FM3 and FM93/2 cells compared with free peptide-expanded T-cells (figure 4G). This is despite the higher frequency of specific T-cells in the free peptide-expanded T-cell product from patient MM1.06-E3, further supporting the improved functional capacity of Ag-scaffold-expanded T-cells. All T-cell products showed minimal killing of HLA-A0201-negative FM45 melanoma cells, indicating that the killing was primarily mediated by tumor-antigens displayed on HLA-A0201 (online supplemental figure 4B).

The highly flexible composition of Ag-scaffolds makes the technology applicable in many disease settings. The range of antigen-specific T-cell populations that can be targeted by Ag-scaffolds, is only limited by availability of cognate pMHCs. Accordingly, the Ag-scaffold technology also allows expansion of previously identified neoantigen-specific T-cells up to several 1000-fold in PBMCs from bladder cancer patients[49] (online supplemental figure 4C). In addition, Ag-scaffolds efficiently expand tumor-specific TILs from tumor fragment or digest from patients with melanoma (online supplemental figure 4D).

Taken together, this shows that Ag-scaffold-directed expansion yields a greater number of tumor-specific T-cells, with desired phenotypic characteristics of self-renewal and improved tumor cell killing, when compared to conventional expansion with free peptide and cytokines.

Expansion of tumor-specific T-cells from patient PBMCs using a multitargeting shared melanoma Ag-scaffold

In order to design a multitargeting 'off-the-shelf' Ag-scaffold for ACT in melanoma, we identified a set of HLA-A0201-restricted TSA-derived epitopes most commonly recognized by T-cells in retrospective screening of either TILs or PBMCs from a total of 87 HLA-A0201-positive patients with metastatic melanoma.[9 50 51] Patients were screened for T-cell reactivity using overlapping libraries of 145–168 HLA-A0201-restricted TSAs using either combinatorial encoded or barcode-labeled pMHC multimers,[28 29] from which we selected the top 30 most frequently recognized TSAs in the evaluated patients (figure 5A, online supplemental figure 5A). T-cell recognition of at least one of the 30 selected TSAs was found in >80% of patients, with T-cell recognition of >3 TSAs in >30% of patients. As a single epitope, MAGE-A2 LVHFLLLKY was by far the most detected specificity, with T-cell reactivity observed in >31% of patients (figure 5A). Thus, combining 30 Ag-scaffolds targeting the selected TSA-specific T-cell populations, would allow expansion of TSA-specific T-cells in the majority of patients with HLA-A0201-positive melanoma (online supplemental figure 2B,C).

Using a set of multitargeting shared melanom a Ag-scaffolds, we could significantly expand TSA-specific T-cells more than 10-fold from six out of nine patients with HLA-A0201-positive metastatic melanoma (MM1, figure 5B–D). When screening Ag-scaffold-expanded T-cells for reactivity against the individual 30 TSAs using combinatorial encoded pMHC multimers, the same six patients showed reactivity against at least two of the 30 TSAs, with patient MM1.06 and MM1.32 showing reactivity against eight and seven, respectively (figure 5E). TCR sequencing of Ag-scaffold-expanded T-cells from MM1.06 and

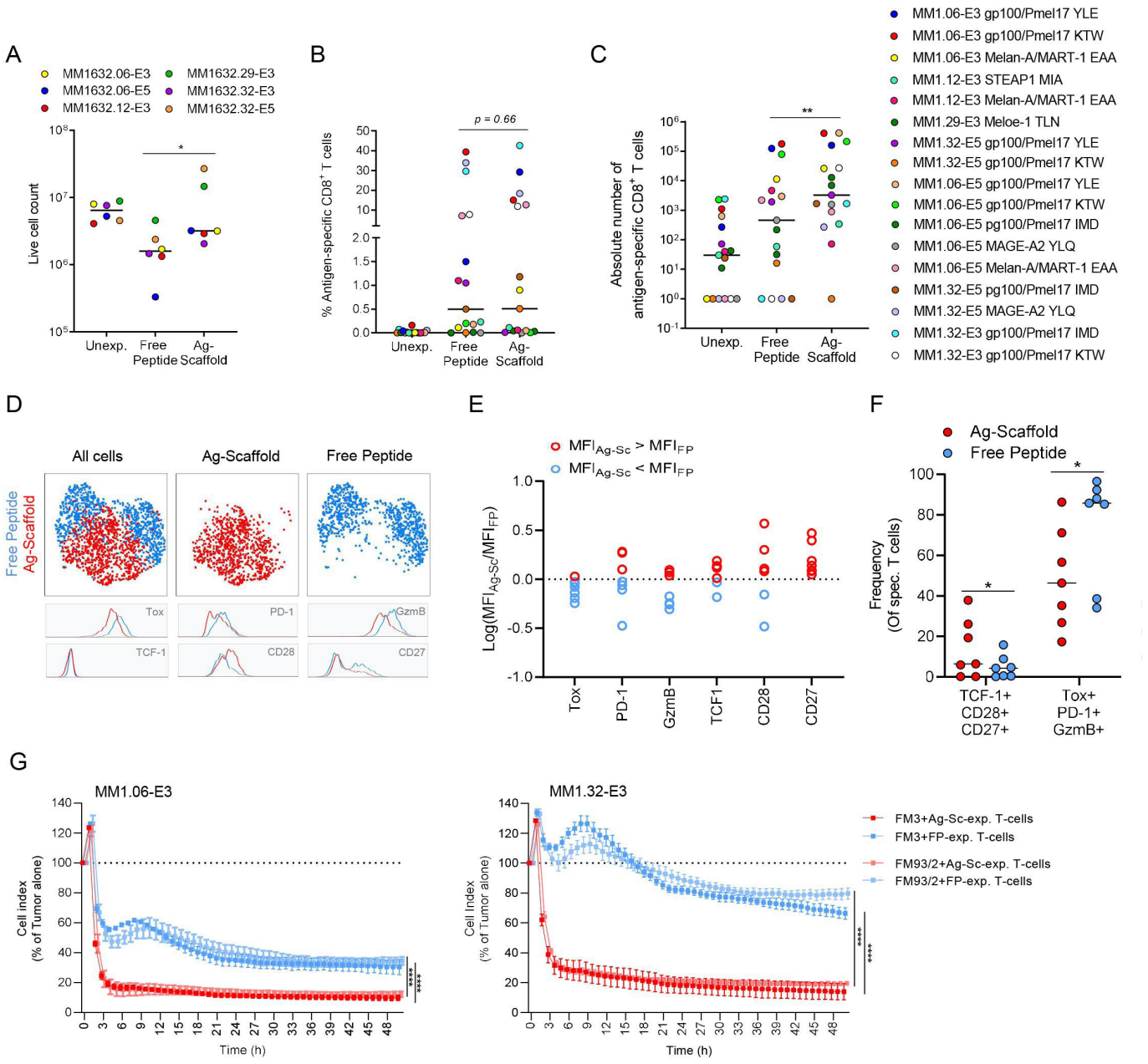

Figure 4 Ag-scaffolds efficiently expand tumor-specific T-cells and render a multifunctional T-cell product. (A) Number of viable cells at culture initiation (Unexp.) and following 2-week expansion with either dextran:pMHC:IL-2:IL-21 Ag-scaffold or free peptide-based expansion, adding specific peptide, IL-2 and IL-21 directly to the media, targeting melanoma shared antigens in six patients with metastatic melanoma samples (PBMC). (B) Post-expansion frequency and (C) number of tumor-specific T-cells (seven specificities) from 17 expansions from six patients with metastatic melanoma samples, with either dextran:pMHC:IL-2:IL-21 Ag-scaffold or free peptide-based expansion adding specific peptide, IL-2 and IL-21 to the media. (D) UMAP plot of HLA-A0201 gp100/Pmel17 YLE-specific T-cells expanded from patient MM1.06-E5 with either Ag-scaffold or free peptide. Specific T-cells were identified by tetramer-staining and stained with an antibody panel including markers of self-renewing (TCF-1, CD28, CD27) and terminally differentiated/exhausted (Tox, PD-1, GzmB) T-cells. The expression of these markers on Ag-scaffold (red) and free peptide (blue)-expanded T-cells were compared in MFI histograms. (E) Extended phenotypic comparison between Ag-scaffold and free peptide-expanded T-cells (Log($MFI_{Ag\text{-}Sc}/MFI_{FP}$) across two different tumor-specific T-cell populations expanded from four patient samples. (F) Frequency of TCF-$1^{+}CD28^{+}CD27^{+}$ and PD-$1^{+}GzmB^{+}Tox^{+}$ T-cells out of antigen-specific T-cells expanded with either Ag-scaffold and free peptide. (G) Survival of A0201-positive FM3 and FM93/2 melanoma tumor cells (Cell Index as a relative measure of impedance presented as % of tumor alone) on co-culture with Ag-scaffold (light/dark red) or free peptide-expanded (light/dark blue) tumor-specific T-cells from MM1.06- and 32-E3 in a 4:1 E:T ratio. Duplicate-means were compared in a paired, non-parametric Wilcoxon test and $p<0.05$ and $p<0.01$ are indicated as * and **, respectively. Ag-scaffolds, antigen-presenting scaffold; GzmB, granzyme B; HLA, human leukocyte antigen, IL, interleukin; MFI, mean fluorescence intensity; PBMCs, peripheral blood mononuclear cells; PD-1, Programmed cell death protein 1; pMHC, peptide-MHC; Tox, Thymocyte selection-associated high mobility group box protein; UMAP, uniform manifold approximation and projection.

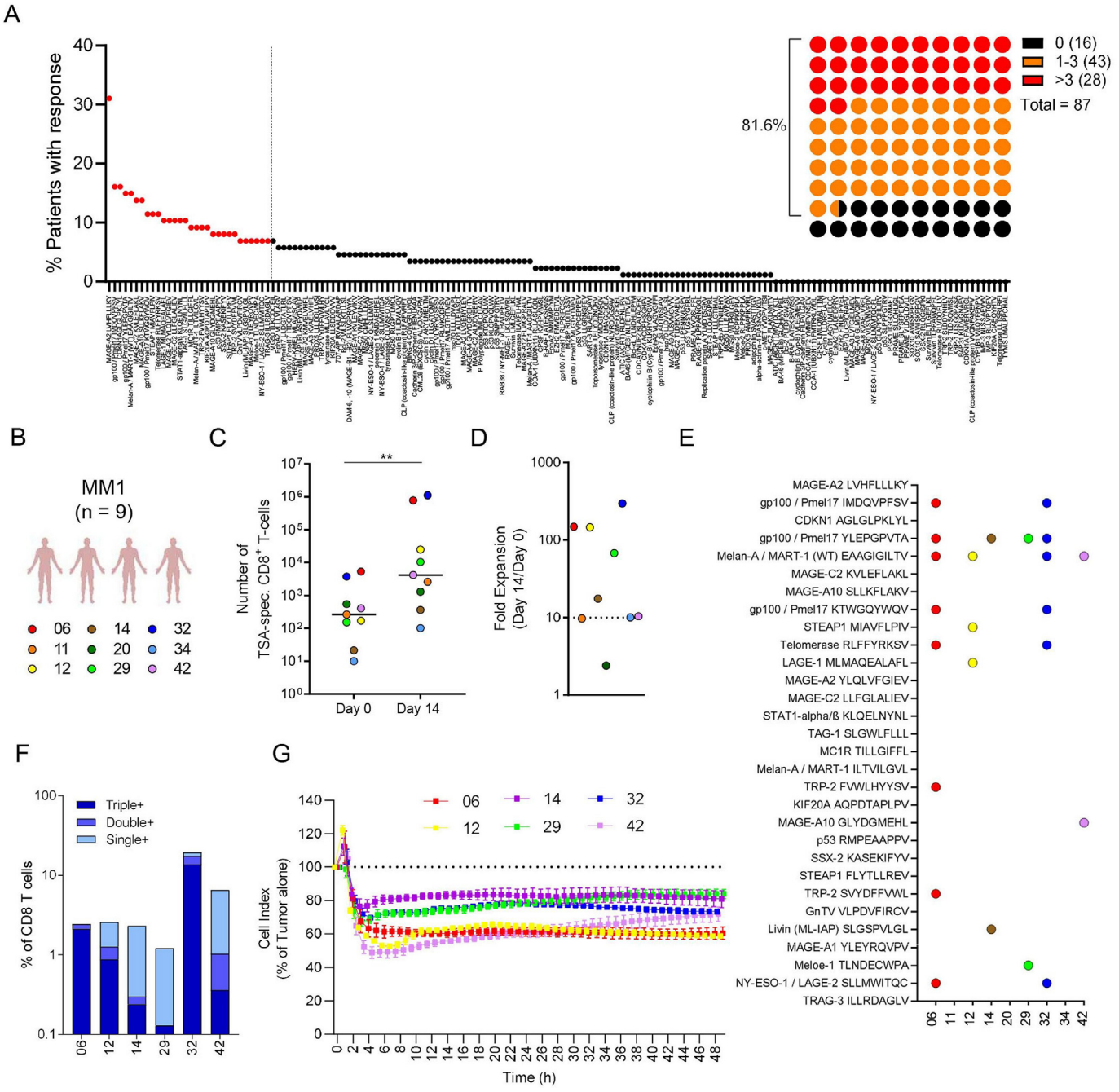

Figure 5 Expansion of tumor-specific T-cells using a multitargeting shared melanoma Ag-scaffold. (A) Percentage of patients showing reactivity towards the library of HLA-A0201-restricted TSAs. Marked in red are the top 30 most commonly recognized shared melanoma antigens among the evaluated patients. To the right, a schematic representation showing that 43/87 (~49%) patients showed reactivity against 1–3 of the selected 30 shared melanoma antigens and 28/87 (~32%) showed reactivity against >3. (B) PBMCs from a cohort of nine patients with metastatic melanoma (MM1) were expanded with the multitargeting shared melanoma Ag-scaffold, comprizing 30 Ag-scaffolds carrying the 30 selected TSAs on HLA-A0201. (C) Number of TSA-specific T-cells pre-expansion (Day 0) and post-expansion (Day 14) were compared in a paired, non-parametric Wilcoxon test and $p<0.01$ is indicated as **. (D) Fold expansion (FE = Day 14/Day0). (E) Post-expansion T-cell populations among the 30 shared melanoma antigens. (F) Frequency of Triple+, Double+ and Single+for IFN-γ, TNF-α and CD107a+ out of the total $CD8^+$ T-cell population on challenge with cognate-antigen (identified in Figure 6E) in the six patients with successful expansion of melanoma-specific T-cells. (G) Survival of HLA-A0201-positive FM93/2 melanoma tumor cells (Cell Index as a relative measure of impedance presented as % of tumor alone) when co-cultured with Ag-scaffold-expanded T-cells from the six patients with melanoma in a 4:1 E:T ratio. Ag-scaffolds, antigen-presenting scaffold; E:T, effector:target; HLA, human leukocyte antigen; IFN, Interferon; PBMCs, peripheral blood mononuclear cells; TNF, tumor necrosis factor; TSA, tumor shared antigen.

MM1.32 revealed that the TSA-specific T-cell population comprise of 58 and 32 clones, although a smaller set of dominating clones contribute to 81.8% and 90.5% of the TCR recognition, respectively (online supplemental figure 5C). TCR sequencing of Ag-scaffold-expanded Gp100/Pmel17 YLE-specific and IMD-specific T-cells from MM1.32 showed that multiple clonal T-cell populations are maintained throughout the expansion period (online supplemental figure 5D).

To investigate the functionality of TSA-specific T-cells, Ag-scaffold-expanded T-cells from the six patients showing reactivity, were challenged with a pool of cognate TSA-derived peptides corresponding to the ones identified in figure 5E. All patients showed some level of functional reactivity upon antigen-challenge measured by expression of TNFα, IFNγ and CD107a (figure 5F), and the frequency of triple-positive correlated with the frequency of melanoma-specific T-cells among the six patients (online supplemental figure 5B). Expanded TSA-specific T-cells from five of the six patients showed capacity to kill FM93/2 cells in co-culture, to a greater extent than HLA-A0201-negative FM45 cells (figure 5G, online supplemental figure 6A).

Strengthening its clinical applicability, the multitargeting shared melanoma Ag-scaffold showed similar efficiency in one additional cohort of 10 patients with HLA-A0201-positive melanoma (MM2), with 70% of patients showing >10-fold expansion and 9 of 10 patients displayed capacity to kill FM3 cells in co-culture (online supplemental figure 6B–F).

Taken together, we identified the top 30 most common TSAs in a cohort of patients with metastatic melanoma, allowing us to design a shared multitargeting Ag-scaffold product for expansion of TSA-specific T-cells from peripheral blood PBMCs from HLA-A0201-positive patients. This multitargeting shared melanoma Ag-scaffold can expand TSA-specific T-cells from peripheral blood PBMCs in 68% of evaluated patients, yielding a multifunctional T-cell product with in vitro tumor cell killing capacity.

DISCUSSION

Adoptive transfer of ex vivo expanded T-cells has emerged as a powerful tool in the treatment of cancer and viral infections. Clearly, response to ACT is dependent on the quality of the final T-cell infusion product. This should ideally contain a high frequency of T-cells with relevant specificity and capacity to persist, proliferate and respond to their targets in vivo.[52 53] A major challenge in ACT is to expand T-cells while maintaining their capacity to self-renew and persist upon infusion.[5 6] Depending on the strength and quality of stimulatory signals received during expansion, T-cells transition through progressive stages of differentiation characterized by a stepwise loss of functional and therapeutic potential.[54 55] Thus, inducing a strong activation signal should not be the focus when designing technologies for antigen-specific T-cell expansion. Instead, appropriate stimulation levels, that ensure desired T-cell activation while preventing exhaustion, should be achieved.

Here we present a new, simple and easily modifiable technology to selectively expand antigen-specific T-cells ex vivo. The Ag-scaffold consists of a commercially available streptavidin-dextran conjugate backbone to which any molecule, carrying a biotinylation, can be attached via strong non-covalent interaction. By co-attaching specific pMHCs and stimulatory molecules, the Ag-scaffold can selectively deliver stimulation to virus-specific or tumor-specific T-cells in ACT strategies for treatment of infectious diseases or cancer, respectively. Reciprocally, Ag-scaffolds can be adapted to deliver inhibitory signals to self-reactive T-cells in autoimmune disease, by co-attachment of pMHC and inhibitory molecules. Besides targeting specific T-cells via attached pMHC, Ag-scaffolds can be modified to target a range of other cell types simply by attaching alternative ligands/antigens, for example, CAR-T cells (CD19) and Mucosal-associated invariant T cells (MAIT cells) (MR-1).

Dextran is a very attractive biomaterial, as it is a biodegradable polymer producing biocompatible degradation products that are not accumulated in the body. Accordingly, dextrans are already widely used in clinical settings, for example, as plasma volume expanders and anticoagulants.[12] Ag-scaffolds are degraded during culture with T-cells and are no longer detectable in the washed cell product. Thus, unlike other aAPCs, this technology bypasses the need for a removal step prior to clinical use, which is both costly and adds additional stress and handling of the T-cell product.[14] Furthermore, Ag-scaffolds could potentially also be applied to directly target T-cells in vivo to bypass the need for ex vivo expansion or to support transferred T-cells after ACT. Supportively, filamentous or rod-like particles like the Ag-scaffold, show longer in vivo circulation times compared with spherical particles.[56]

Natural APCs have the ability to conform to the T-cell surface topography, enabling dynamic movement of receptor-ligand complexes and proper synapse formation. Thus, aAPC shape is a key parameter that impacts T-cell activation. Compared with spherical bead-based or nanoparticle-based aAPCs, elongated aAPCs have been shown to provide increased contact with T-cells resulting in increased expansion capacity.[57] The flexible nature of linear dextran enables efficient multivalent binding between dextran-bound molecules and the target T-cell. In another polymer-based aAPC strategy, it was observed that multivalent interaction is required for optimal formation of artificial immunological synapse between the T-cells and aAPC and intracellular signaling on T-cell activation.[58] This strategy is structurally similar to the Ag-scaffold technology with a streptavidin-decorated poly(isocyano peptides) backbone, however, its use is currently limited to polyclonal T-cell expansion via presentation of αCD3 and αCD28 antibodies.[58–60]

Only few alternative aAPC strategies have succeeded to directly target T-cells in a pMHC-dependent fashion. One

such strategy is biomaterial-based APC-mimetic scaffolds (APC-ms), comprizing supported lipid bilayers formed on high aspect ratio mesoporous micro-rods (SLB-MSRs), which enables presentation of both surface (αCD28/αCD3 or pMHC) and soluble (IL-2) cues to T-cells.[61] Moreover, similar properties were obtained with an artificial T-cell stimulating matrix (aTM) comprizing a hyaluronic acid-based hydrogel conjugated with pMHC and αCD28.[62] These strategies are functionally comparable to Ag-scaffolds and share many of its desired properties, however, they represent far more complex structures. The preparation of aTM and MSRs and liposomes preceding APC-ms assembly is indeed laborious and time-consuming.[62–64] In addition, these biomaterials have no previous records of clinical use.

Comparing a wide range of Ag-scaffolds with different cytokine and co-stimulatory molecule combinations, we identified an Ag-scaffold carrying pMHC, IL-2 and IL-21 that had superior capacity to generate a T-cell product with a high frequency of antigen-specific and multifunctional $CD8^+$ T-cells; a feature associated with enhanced quality of subsequent T-cell response and protection.[34] IL-2 is a powerful T-cell growth factor and has been a key cytokine for T-cell expansion preceding ACT. However, IL-2 also drives collateral expansion of regulatory T cells (Tregs) and progressive effector differentiation, which are factors known to limit in vivo persistence and ACT response.[65] IL-21 is a member of the common γ-chain family of cytokines that share the γ-chain receptor (CD132) with IL-2. Although a less potent T-cell growth factor compared with IL-2, IL-21 provides a range of favorable features in the context of immunotherapy, including suppression of Treg expansion and enhancement of antigen-specific T-cell memory formation.[66–69] In combination with IL-2, IL-21 increases TCR-dependent proliferation to a level beyond that with IL-2 alone.[70] Consequently, the concentration of IL-2 required for optimal T-cell expansion can be lowered in the presence of IL-21, which promotes development of early memory T-cells, rather than exhausted effector phenotypes.[65] In addition, IL-21 opposes the negative impact of IL-2 on T-cell differentiation in ACT and tumor-antigen vaccination in vivo, resulting in the preservation of an early memory phenotype among antigen-stimulated $CD8^+$ T-cells and enhanced antitumor efficacy in melanoma-engrafted mice, when comparing to single therapy with either IL-21 or IL-2 alone.[71 72]

The Ag-scaffold design enables the simultaneous delivery of IL-2 and IL-21 to targeted antigen-specific T-cells, providing them with a fine-tuned and orchestrated T-cell activating signal. Consistently, Ag-scaffold-expanded T-cells display a favorable phenotype, with increased levels of TCF-1, a transcription factor that plays an important role in memory formation and maintenance,[73] along with co-stimulatory receptors CD27 and CD28, compared with conventional free peptide-based expansion, where specific peptide and cytokines are added directly to the culture in a non-orchestrated manner. CD27 and CD28 are found on the majority of memory T-cells and their expression is gradually lost as cells become terminally differentiated.[54] Accordingly, CD27 and CD28-expression on infused T-cells has been associated with increased persistence of infused cells and objective responses to ACT.[74 75] On the other hand, Ag-scaffold-expanded T-cells showed lower levels of markers of late differentiation and exhaustion including high level expression of the combination of transcriptional regulator Tox, PD-1 and the cytotoxic molecule GzmB,[55] indicating that the Ag-scaffold provides a higher quality of stimulation during expansion hereby limiting T-cell exhaustion.

Finally, by simply combining Ag-scaffolds with different pMHCs, multiple specific T-cell populations can be expanded simultaneously from a single culture. Since each peptide is equally represented on individual Ag-scaffolds in the context of MHC, competition for presentation is eliminated. Since optimal antitumor responses require simultaneous targeting of multiple tumor antigens, this is an important feature of the Ag-scaffold technology.[76] The features of Ag-scaffold-expanded T-cells makes the technology attractive for evaluation in clinical settings. Here we demonstrate an "off-the-shelf" strategy targeting metastatic melanoma, in which multiple Ag-scaffolds, containing the most commonly recognized TSA epitopes in a cohort of patients with HLA-A0201-positive melanoma, were combined. Using the Ag-scaffold product, we could expand TSA-specific $CD8^+$ T-cells with tumor cell killing-capacity from the majority of evaluated patient PBMCs. In a similar manner, Ag-scaffolds can be assembled with an alternative selection of producible HLAs and relevant epitopes allowing expansion of ACT products for a range of patients and indications. Translated into clinical practice; this allows the generation of a T-cell product for ACT containing Ag-scaffold-expanded TSA-specific $CD8^+$ T-cells directly from a patient blood sample.

This is an attractive alternative to TIL-ACT, in particular when surgical resection of a tumor lesion is not possible, or the TIL culture fails to provide a usable T-cell product. Additionally, a recent screen in patients with melanoma, had a subgroup of patients with detected neoantigen-specific T-cells in the blood pre-ACT and not in the TIL infusion product, indicating that these cells were either not present in the resected tumor lesion or not expandable ex vivo.[52] In both cases, a patient-tailored Ag-scaffold for expanding detected neoantigen-specific T-cell populations from patient PBMCs could be an alternative strategy to generate a cancer-specific T-cell infusion product.

Taken together, we demonstrate a simple, easily modifiable, and clinically relevant new technology for antigen-specific T-cell expansion. While T-cell therapies are entering standard clinical care in solid tumor oncology, our strategy represents a promising alternative to both TIL-ACT and other aAPC technologies.

Author affiliations
[1]Department of Health Technology, Technical University of Denmark, Lyngby, Denmark
[2]PokeAcell Aps, BioInnovation Institute, Copenhagen, Denmark
[3]National Center for Cancer Immune Therapy (CCIT-DK), Department of Oncology, Herlev Hospital, Herlev, Denmark

[4]NMI Natural and Medical Science Institute, University of Tübingen, Tubingen, Germany
[5]Deptartment of Medicine, Memorial Sloan Kettering Cancer Center, New York, New York, USA
[6]National Center for Cancer Immune Therapy (CCIT-DK), Department of Oncology, Herlev Hospital, Copenhagen, Denmark

Twitter Arianna Draghi @AriannaDraghi and Marco Donia @doniamarco

Acknowledgements We thank Adaptive Biotechnologies for providing the TCR sequencing data presented in online supplemental figure S5.

Contributors SAT, MSF, VMR, and SRH designed the research and wrote the manuscript. UKH, MO, AT, AWPJ, MK, AKB, KKM, GNA, JSHT, CH, TT, CS, and SF contributed to experiments and analysis. JWK, AHK, ÖM, AD, SNJ, MD, and IMS provided important materials, methods and advice. SRH is responsible for the overall content as the guarantor.

Funding This study was funded by the Lundbeck Foundation fellowship (grant no. R190-2014-4178), The Danish Ministry of Research and Education (grant: Empowering cancer immunotherapy in Denmark), The Innovation Fund Denmark (grant no: 9122-00084), The European Research Council, ERC StG NextDART, and the Independent Research Fund Denmark (grant: Sapere Aude, 4004-00422B).

Competing interests SRRH is the co-founder of PokeAcell, with license to SRRH co-invented patents (EP2017/083862 and EP3810188A1); further, SRRH is the co-inventor of patents WO2015185067 and WO2015188839 for the barcoded MHC technology that is licensed to Immudex. The remaining authors have no conflicts of interest in the context of the present study.

Patient consent for publication Not applicable.

Ethics approval All patient material was collected with approval from the local Scientific Ethics Committee and written informed consent was obtained from all participants according to the Declaration of Helsinki.

Provenance and peer review Not commissioned; externally peer reviewed.

Data availability statement All data relevant to the study are included in the article or uploaded as supplementary information. All data is present in this research article and Supplementary Materials, which includes Supplementary Figure S1–S5 and Supplementary Table 1–3.

ORCID iDs
Agnete W P Jensen http://orcid.org/0000-0001-8868-7481
Mohammad Kadivar http://orcid.org/0000-0003-1499-191X
Christian Schmess http://orcid.org/0000-0003-4883-2642
Anders Handrup Kverneland http://orcid.org/0000-0002-9883-936X
Arianna Draghi http://orcid.org/0000-0002-5894-6750
Marco Donia http://orcid.org/0000-0003-4966-9752
Sine Reker Hadrup http://orcid.org/0000-0002-5937-4344

REFERENCES

1 Ellis GI, Sheppard NC, Riley JL. Genetic engineering of T cells for Immunotherapy. *Nat Rev Genet* 2021;22:427–47.
2 van den Berg JH, Gomez-Eerland R, van de Wiel B, *et al*. Case report of a fatal serious adverse event upon administration of T cells Transduced with a MART-1-specific T-cell receptor. *Mol Ther* 2015;23:1541–50.
3 Takahama Y. Journey through the thymus: Stromal guides for T-cell development and selection. *Nat Rev Immunol* 2006;6:127–35.
4 Rohaan MW, Borch TH, van den Berg JH, *et al*. Tumor-infiltrating lymphocyte therapy or Ipilimumab in advanced Melanoma. *N Engl J Med* 2022;387:2113–25.
5 Powell DJ Jr, Dudley ME, Robbins PF, *et al*. Transition of late-stage Effector T cells to Cd27+ Cd28+ tumor-reactive Effector memory T cells in humans after adoptive cell transfer therapy. *Blood* 2005;105:241–50.
6 Li Y, Liu S, Hernandez J, *et al*. MART-1-specific Melanoma tumor-infiltrating lymphocytes maintaining Cd28 expression have improved survival and expansion capability following Antigenic Restimulation in vitro. *J Immunol* 2010;184:452–65.
7 Donia M, Kjeldsen JW, Andersen R, *et al*. PD-1(+) Polyfunctional T cells dominate the periphery after tumor-infiltrating lymphocyte therapy for cancer. *Clin Cancer Res* 2017;23:5779–88.
8 Simoni Y, Becht E, Fehlings M, *et al*. Bystander Cd8(+) T cells are abundant and Phenotypically distinct in human tumour infiltrates. *Nature* 2018;557:575–9.
9 Andersen RS, Thrue CA, Junker N, *et al*. Dissection of T-cell antigen specificity in human Melanoma. *Cancer Res* 2012;72:1642–50.
10 Ahmadzadeh M, Johnson LA, Heemskerk B, *et al*. Tumor antigen-specific Cd8 T cells infiltrating the tumor express high levels of PD-1 and are functionally impaired. *Blood* 2009;114:1537–44.
11 Scott AC, Dündar F, Zumbo P, *et al*. TOX is a critical regulator of tumour-specific T cell differentiation. *Nature* 2019;571:270–4.
12 Dubniks M, Persson J, Grände P-O. Comparison of the plasma volume-expanding effects of 6% dextran 70, 5% albumin, and 6% HES 130/0.4 after hemorrhage in the guinea pig. *J Trauma* 2009;67:1200–4.
13 Dustin ML. What counts in the immunological synapse? *Mol Cell* 2014;54:255–62.
14 Hasan AN, Selvakumar A, O'Reilly RJ. Artificial antigen presenting cells: an off the shelf approach for generation of desirable T-cell populations for broad application of adoptive Immunotherapy. *Adv Genet Eng* 2015;4:130.
15 Schluck M, Hammink R, Figdor CG, *et al*. Biomaterial-based activation and expansion of tumor-specific T cells. *Front Immunol* 2019;10:931.
16 Porter DL, Levine BL, Bunin N, *et al*. A phase 1 trial of donor lymphocyte infusions expanded and activated ex vivo via Cd3/Cd28 Costimulation. *Blood* 2006;107:1325–31.
17 Zappasodi R, Di Nicola M, Carlo-Stella C, *et al*. The effect of artificial antigen-presenting cells with Preclustered anti-Cd28/-Cd3/-LFA-1 Monoclonal antibodies on the induction of ex vivo expansion of functional human antitumor T cells. *Haematologica* 2008;93:1523–34.
18 Jin C, Yu D, Hillerdal V, *et al*. Allogeneic lymphocyte-licensed Dcs expand T cells with improved antitumor activity and resistance to oxidative stress and immunosuppressive factors. *Mol Ther Methods Clin Dev* 2014;1:14001.
19 Li Y, Kurlander RJ. Comparison of anti-Cd3 and anti-Cd28-coated beads with soluble anti-Cd3 for expanding human T cells: differing impact on Cd8 T cell phenotype and responsiveness to Restimulation. *J Transl Med* 2010;8:104.
20 Ichikawa J, Yoshida T, Isser A, *et al*. Rapid expansion of highly functional antigen-specific T cells from patients with Melanoma by Nanoscale artificial antigen-presenting cells. *Clin Cancer Res* 2020;26:3384–96.
21 Perica K, Bieler JG, Schütz C, *et al*. Enrichment and expansion with Nanoscale artificial antigen presenting cells for adoptive Immunotherapy. *ACS Nano* 2015;9:6861–71.
22 Isser A, Livingston NK, Schneck JP. Biomaterials to enhance antigen-specific T cell expansion for cancer Immunotherapy. *Biomaterials* 2021;268:S0142-9612(20)30830-9.
23 Pawelec G, Marsh SG. ESTDAB: a collection of Immunologically characterised Melanoma cell lines and Searchable Databank. *Cancer Immunol Immunother* 2006;55:623–7.
24 Hadrup SR, Toebes M, Rodenko B, *et al*. High-throughput T-cell EPITOPE discovery through MHC peptide exchange. *Methods Mol Biol* 2009;524:383–405.
25 Rodenko B, Toebes M, Hadrup SR, *et al*. Generation of peptide-MHC class I complexes through UV-mediated ligand exchange. *Nat Protoc* 2006;1:1120–32.
26 Saini SK, Tamhane T, Anjanappa R, *et al*. Empty peptide-receptive MHC class I molecules for efficient detection of antigen-specific T cells. *Sci Immunol* 2019;4:eaau9039.
27 Andersen RS, Kvistborg P, Frøsig TM, *et al*. Parallel detection of antigen-specific T cell responses by Combinatorial Encoding of MHC Multimers. *Nat Protoc* 2012;7:891–902.

28 Hadrup SR, Bakker AH, Shu CJ, *et al*. Parallel detection of antigen-specific T-cell responses by multidimensional Encoding of MHC Multimers. *Nat Methods* 2009;6:520–6.
29 Bentzen AK, Marquard AM, Lyngaa R, *et al*. Large-scale detection of antigen-specific T cells using peptide-MHC-I Multimers labeled with DNA Barcodes. *Nat Biotechnol* 2016;34:1037–45.
30 Wu T, Hu E, Xu S, *et al*. clusterProfiler 4.0: A universal enrichment tool for interpreting Omics data. *Innovation (Camb)* 2021;2:100141.
31 Li H, van der Leun AM, Yofe I, *et al*. Dysfunctional Cd8 T cells form a proliferative, dynamically regulated compartment within human Melanoma. *Cell* 2020;181:747.
32 Ke N, Wang X, Xu X, *et al*. The xCELLigence system for real-time and label-free monitoring of cell viability. *Methods Mol Biol* 2011;740:33–43.
33 Betts MR, Brenchley JM, Price DA, *et al*. Sensitive and viable identification of antigen-specific Cd8+ T cells by a flow Cytometric assay for Degranulation. *J Immunol Methods* 2003;281:65–78.
34 Seder RA, Darrah PA, Roederer M. T-cell quality in memory and protection: implications for vaccine design. *Nat Rev Immunol* 2008;8:247–58.
35 Li H, van der Leun AM, Yofe I, *et al*. Dysfunctional Cd8 T cells form a proliferative, dynamically regulated compartment within human Melanoma. *Cell* 2019;176:e18:775–789..
36 Filén S, Lahesmaa R. GIMAP proteins in T-lymphocytes. *J Signal Transduct* 2010;2010:268589.
37 Yánez DC, Ross S, Crompton T. The IFITM protein family in adaptive immunity. *Immunology* 2020;159:365–72.
38 Park I, Son M, Ahn E, *et al*. The Transmembrane Adaptor protein LIME is essential for Chemokine-mediated migration of Effector T cells to Inflammatiory sites. *Mol Cells* 2020;43:921–34.
39 Seo H, González-Avalos E, Zhang W, *et al*. BATF and Irf4 cooperate to counter exhaustion in tumor-infiltrating CAR T cells. *Nat Immunol* 2021;22:983–95.
40 Yan M, Hu J, Yuan H, *et al*. Dynamic regulatory networks of T cell trajectory dissect transcriptional control of T cell state transition. *Mol Ther Nucleic Acids* 2021;26:1115–29.
41 Park CG, Lee SY, Kandala G, *et al*. A novel gene product that couples TCR signaling to Fas(Cd95) expression in activation-induced cell death. *Immunity* 1996;4:583–91.
42 Voisinne G, Gonzalez de Peredo A, Roncagalli R. Cd5, an undercover regulator of TCR signaling. *Front Immunol* 2018;9:2900.
43 Agresta L, Hoebe KHN, Janssen EM. The emerging role of Cd244 signaling in immune cells of the tumor Microenvironment. *Front Immunol* 2018;9:2809.
44 Christiaansen AF, Dixit UG, Coler RN, *et al*. Cd11A and Cd49D enhance the detection of antigen-specific T cells following human vaccination. *Vaccine* 2017;35:4255–61.
45 Brusko TM, Wasserfall CH, Hulme MA, *et al*. Influence of membrane Cd25 stability on T lymphocyte activity: implications for Immunoregulation. *PLoS One* 2009;4:e7980.
46 Kalia V, Sarkar S, Subramaniam S, *et al*. Prolonged Interleukin-2Ralpha expression on virus-specific Cd8+ T cells favors terminal-Effector differentiation in vivo. *Immunity* 2010;32:91–103.
47 Canale FP, Ramello MC, Núñez N, *et al*. Cd39 expression defines cell exhaustion in tumor-infiltrating Cd8(+) T cells-response. *Cancer Res* 2018;78:5175.
48 Gloger A, Ritz D, Fugmann T, *et al*. Mass spectrometric analysis of the HLA class I Peptidome of Melanoma cell lines as a promising tool for the identification of putative tumor-associated HLA epitopes. *Cancer Immunol Immunother* 2016;65:1377–93.
49 Holm JS, Funt SA, Borch A, *et al*. Neoantigen-specific Cd8 T cell responses in the peripheral blood following PD-L1 blockade might predict therapy outcome in metastatic urothelial carcinoma. *Nat Commun* 2022;13:1935.
50 Kvistborg P, Shu CJ, Heemskerk B, *et al*. TIL therapy broadens the tumor-reactive Cd8(+) T cell compartment in Melanoma patients. *Oncoimmunology* 2012;1:409–18.
51 Gaißler A, Meldgaard TS, Heeke C, *et al*. Dynamics of Melanoma-associated EPITOPE-specific Cd8+ T cells in the blood correlate with clinical outcome under PD-1 blockade. *Front Immunol* 2022;13:906352.
52 Kristensen NP, Heeke C, Tvingsholm SA, *et al*. Neoantigen-reactive Cd8+ T cells affect clinical outcome of adoptive cell therapy with tumor-infiltrating lymphocytes in Melanoma. *J Clin Invest* 2022;132.
53 Huang J, Khong HT, Dudley ME, *et al*. Survival, persistence, and progressive differentiation of Adoptively transferred tumor-reactive T cells associated with tumor regression. *J Immunother* 2005;28:258–67.
54 Gattinoni L, Klebanoff CA, Restifo NP. Paths to Stemness: building the ultimate Antitumour T cell. *Nat Rev Cancer* 2012;12:671–84.
55 Kallies A, Zehn D, Utzschneider DT. Precursor exhausted T cells: key to successful Immunotherapy *Nat Rev Immunol* 2020;20:128–36.
56 Zhao Y, Wang Y, Ran F, *et al*. A comparison between sphere and rod nanoparticles regarding their in vivo biological behavior and pharmacokinetics. *Sci Rep* 2017;7:7.
57 Sunshine JC, Perica K, Schneck JP, *et al*. Particle shape dependence of Cd8+ T cell activation by artificial antigen presenting cells. *Biomaterials* 2014;35:269–77.
58 Hammink R, Mandal S, Eggermont LJ, *et al*. Controlling T-cell activation with synthetic Dendritic cells using the Multivalency effect. *ACS Omega* 2017;2:937–45.
59 Mandal S, Hammink R, Tel J, *et al*. Polymer-based synthetic Dendritic cells for Tailoring robust and Multifunctional T cell responses. *ACS Chem Biol* 2015;10:485–92.
60 Mandal S, Eksteen-Akeroyd ZH, Jacobs MJ, *et al*. Rowan therapeutic Nanoworms: towards novel synthetic Dendritic cells for Immunotherapy. *Chem Sci* 2013;4:4168.
61 Cheung AS, Zhang DKY, Koshy ST, *et al*. Scaffolds that mimic antigen-presenting cells enable ex vivo expansion of primary T cells. *Nat Biotechnol* 2018;36:160–9.
62 Hickey JW, Dong Y, Chung JW, *et al*. Engineering an artificial T-cell stimulating matrix for Immunotherapy. *Adv Mater* 2019;31:e1807359.
63 Kim J, Li WA, Choi Y, *et al*. Injectable, spontaneously assembling, inorganic scaffolds modulate immune cells in vivo and increase vaccine efficacy. *Nat Biotechnol* 2015;33:64–72.
64 Li WA, Lu BY, Gu L, *et al*. The effect of surface modification of Mesoporous silica micro-rod scaffold on immune cell activation and infiltration. *Biomaterials* 2016;83:249–56.
65 Kaartinen T, Luostarinen A, Maliniemi P, *et al*. Low Interleukin-2 concentration favors generation of early memory T cells over Effector phenotypes during Chimeric antigen receptor T-cell expansion. *Cytotherapy* 2017;19:S1465-3249(17)30602-3.
66 Albrecht J, Frey M, Teschner D, *et al*. IL-21-treated naive Cd45Ra+ Cd8+ T cells represent a reliable source for producing leukemia-reactive cytotoxic T lymphocytes with high proliferative potential and early differentiation phenotype. *Cancer Immunol Immunother* 2011;60:235–48.
67 Kaka AS, Shaffer DR, Hartmaier R, *et al*. Genetic modification of T cells with IL-21 enhances antigen presentation and generation of central memory tumor-specific cytotoxic T-lymphocytes. *J Immunother* 2009;32:726–36.
68 Li Y, Yee C. IL-21 mediated Foxp3 suppression leads to enhanced generation of antigen-specific Cd8+ cytotoxic T lymphocytes. *Blood* 2008;111:229–35.
69 Kim-Schulze S, Kim HS, Fan Q, *et al*. Local IL-21 promotes the therapeutic activity of Effector T cells by decreasing regulatory T cells within the tumor Microenvironment. *Mol Ther* 2009;17:380–8.
70 Battaglia A, Buzzonetti A, Baranello C, *et al*. Interleukin-21 (IL-21) Synergizes with IL-2 to enhance T-cell receptor-induced human T-cell proliferation and Counteracts IL-2/transforming growth factor-beta-induced regulatory T-cell development. *Immunology* 2013;139:109–20.
71 He H, Wisner P, Yang G, *et al*. Combined IL-21 and low-dose IL-2 therapy induces anti-tumor immunity and long-term curative effects in a murine Melanoma tumor model. *J Transl Med* 2006;4:24.
72 Hinrichs CS, Spolski R, Paulos CM, *et al*. IL-2 and IL-21 confer opposing differentiation programs to Cd8+ T cells for adoptive Immunotherapy. *Blood* 2008;111:5326–33.
73 Utzschneider DT, Charmoy M, Chennupati V, *et al*. T cell factor 1-expressing memory-like Cd8(+) T cells sustain the immune response to chronic viral infections. *Immunity* 2016;45:415–27.
74 Zhou J, Shen X, Huang J, *et al*. Telomere length of transferred lymphocytes correlates with in vivo persistence and tumor regression in Melanoma patients receiving cell transfer therapy. *J Immunol* 2005;175:7046–52.
75 Rosenberg SA, Yang JC, Sherry RM, *et al*. Durable complete responses in heavily pretreated patients with metastatic Melanoma using T-cell transfer Immunotherapy. *Clin Cancer Res* 2011;17:4550–7.
76 Kaluza KM, Kottke T, Diaz RM, *et al*. Adoptive transfer of cytotoxic T lymphocytes targeting two different antigens limits antigen loss and tumor escape. *Hum Gene Ther* 2012;23:1054–64.